

# Convergence of shearing rate $\omega_{E \times B}$ with box size in gradient driven simulation

M. Lippert,<sup>1, a)</sup> F. Rath,<sup>1, b)</sup> and A. G. Peeters<sup>1</sup>

*Physics Department, University of Bayreuth, 95440 Bayreuth, Germany*

(\*Electronic mail: Florian.Rath1@uni-bayreuth.de)

(Dated: 2 January 2023)

The gradient driven simulation of Rath et al.<sup>1</sup> gets revisited. Its is confirmed that the wavelength of the longest wavelength zonal flow mode converges with increased box sizes in radial and binormal direction. Especially the  $E \times B$  staircase structure repeats itself multiple times in the given box size.

This brief communication focuses on continuing the work of Rath et al.<sup>1</sup>. Their paper elaborates on gradient driven flux-tub simulations close to the non-linear threshold and the occurrence of the  $E \times B$  staircase structure and its formation over the simulation. At the end section IV of the Rath et al. paper it was discussed that the circumstances for which the staircase can fully develop, like the change of the longest wavelength with increasing box size, were beyond the scope of the original paper. To gain further insights on whether the staircase structure can fully develop the following brief communication will focus on the effects of the box size on the  $E \times B$  staircase structure and whether the wavelength converges with the box size.

It is known that radially sheared zonal flows play a significant role in nonlinear stabilization in tokamak plasmas.<sup>2-4</sup>. Through advection on the sheared zonal flows the turbulent structure in plasma gets deformed and tilted, which causes an  $E \times B$  nonlinearity.<sup>3,5,6</sup> The strength of the shearing process is the  $E \times B$  shearing rate  $\omega_{E \times B}$  which is the radial derivative of the advecting zonal flow velocity.<sup>5,7</sup> The shearing rate  $\omega_{E \times B}$  is defined as

$$\omega_{E \times B} = \frac{1}{2} \frac{\partial^2 \langle \Phi \rangle}{\partial \psi^2} \quad (1)$$

where  $\langle \Phi \rangle$  is the zonal electrostatic potential and  $\psi$  the radial coordinate that labels the flux surfaces.<sup>8,9</sup> It was shown that the nonlinear threshold for turbulence is directly related to shear stabilization.<sup>4</sup> The shear stabilization is often expressed in the empirical Waltz rule  $\omega_{E \times B} \sim \gamma$ ,<sup>7,10</sup> where  $\gamma$  is defined as the maximum linear growth rate in the unstable mode. The discovered zonal flows, also known as  $E \times B$  staircase<sup>11</sup>, exhibit amplitudes, which satisfy the stabilization criteria in terms of the  $E \times B$  shearing rate. For a fully developed staircase structure the  $E \times B$  shearing rate  $\omega_{E \times B} = \gamma$ .<sup>1,8</sup>

This paper covers the increase of the box size in radial direction and in binormal direction with periodic boundary conditions for the box itself. Which box size was used can be

seen in each graphic in form of  $N_R \times N_B$ , where  $N_R$  stands for the times the radial box size was increased and  $N_B$  for the binormal box size. To validate a stabilized turbulence and if the  $E \times B$  Staircase structure has fully developed a closer look at the long wavelength zonal flow mode  $|\hat{\omega}_{E \times B}|_{k_i}$  is necessary. The long wavelength zonal flow mode is the absolute of the Fourier transform of the shearing rate  $\omega_{E \times B}$  for each time step, where  $k_i$  is the wave vector connected to the long wavelength zonal flow mode with index  $i$  and is defined as following

$$k_i = \frac{2\pi i}{l_\psi} \quad (2)$$

with  $l_\psi$  as the length of the box size. In addition, the maximum amplitude of the long wavelength zonal flow mode  $|\hat{\omega}_{E \times B}|_{k_i} = \gamma$ .<sup>1</sup> It is important that only for one wave vector  $k_i$  the zonal mode reaches its maximum amplitude any other mode has to be close by zero. The mode with the maximum amplitude is called the longest wavelength zonal mode.

The plasma parameters are closely modelled after those in Rath et al.<sup>1</sup> with the cyclone base case. The resolution "Standard resolution with 6th order (S6)" from Ref 1 was used and is given in Table I with changes in  $N_{v_\parallel}$  from 64 grid points to 48 to reduce the runtime of simulations. Simulations showed no effect of the correction in grid points on the produced results. Furthermore, the gradient length  $R/L_T$  was set to the value 6.0 close to the finite heat flux threshold shown in Fig. 4 in Rath et al.<sup>1</sup>. The simulations are performed with the flux tube version of the non-linear gyro-kinetic code GKW<sup>12</sup> with periodic boundary conditions and circular geometry. Further information regarding the simulation can be found in Ref 1.

	$N_m$	$N_x$	$N_s$	$N_{v_\parallel}$	$N_\mu$	$D$	$v_d$	$D_{v_\parallel}$	$D_x$	$D_y$	Order	$k_y \rho$	$k_x \rho$
S6	21	83	16	48	9	1	$ v_\parallel $	0.2	0.1	0.1	6	1.4	2.1

TABLE I: Resolution used in this paper for further information read Rath et al.<sup>1</sup>

The data is normalized with the heat conduction coefficient  $\chi$  in gyro-Bohm units ( $\rho^2 v_{th}/R$ ), where  $\rho = m_i v_{th}/eB$  is the ion Larmor radius,  $v_{th} = \sqrt{2T/m_i}$  is the thermal velocity,  $T$  the background temperature,  $e$  is the unit charge and  $R$  is the major radius.

<sup>a)</sup>Repository of this work:

<https://github.com/ManeLippert/Bachelorthesis-Shearingrate-Wavelength>

<sup>b)</sup>Author to whom correspondence should be addressed:

Florian.Rath1@uni-bayreuth.de

At the beginning the box size was only increased in radial direction with values for  $N_R = 1, 2, 3, 4$ . The simulations show that the longest wavelength zonal mode is connected with  $N_R$  in terms of index  $i = N_R$ . This behavior can be seen in Fig. 2 where the longest wavelength zonal mode for the box size  $1 \times 1$  has the wave vector  $k_1$ , for  $2 \times 1$  the wave vector  $k_2$  and so on. Despite numerical dissipation of the simulation producing an unlikelihood of turbulence stabilization, it may still stabilize after the simulation is run for a longer amount of time.<sup>1</sup>

Furthermore, it is visible that the longest wavelength zonal mode reaches its maximum amplitude (Fig. 2 (b)) when the turbulence is stabilized (Fig. 2 (a)) but further investigation yields the result that the simulations has not stabilized yet. For example for the box size  $3 \times 1$  the turbulence has not been stabilized between [28000, 31000] normalized time units although the heat conduction coefficient  $\chi$  subdued. This can be observed in Fig. 1 where for [28000, 31000] normalized time units the staircase structure has a jump at 40 normalized radial coordinates. In comparison, an unstable staircase structure has the form of a Sawtooth wave also visible in Fig. 1 for [10000, 12000] normalized time units. This occurrence is due to the previously mentioned condition that only one zonal mode has a maximal amplitude while any other mode has an amplitude close to zero. So as additional verification process one could visualize the shearing rate  $\omega_{E \times B}$  to determine whether the staircase structure has fully developed.

After the turbulence is stabilized and the longest wavelength zonal mode has developed the wavelength of the shearing rate  $\omega_{E \times B}$  converges with the box size. The E  $\times$  B stair-

case structure does repeat itself exactly  $N_R$  times. In Fig. 3 shows how the wavelength converges for different box sizes for different time intervals and the for this paper significant staircase structure repetition pattern. This can be linked to the wave vector of the longest wavelength zonal mode, for example for the box size  $2 \times 1$  the wave vector would be  $k_2$  (Fig. 2(b)) and the staircase structure repeats itself 2 times which shows a convergence of the structure to the box size. It is also visible that the Waltz rule applies for radially increased box sizes as well. Note that for clearer visibility the staircase structure for box size  $1 \times 1$  and for  $4 \times 1$  got shifted to the left in Fig. 3 so that the staircase structures do overlapped. This shift does not affect the physical result because of the applied periodic boundary conditions of the box.

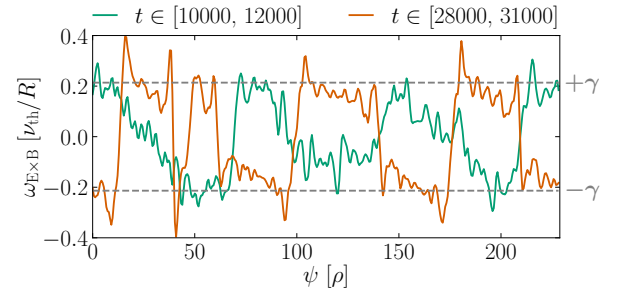


FIG. 1: Shearing rate  $\omega_{E \times B}$  for different time intervals in which heat conduction is almost zero but the E  $\times$  B staircase has not fully developed for box size  $3 \times 1$

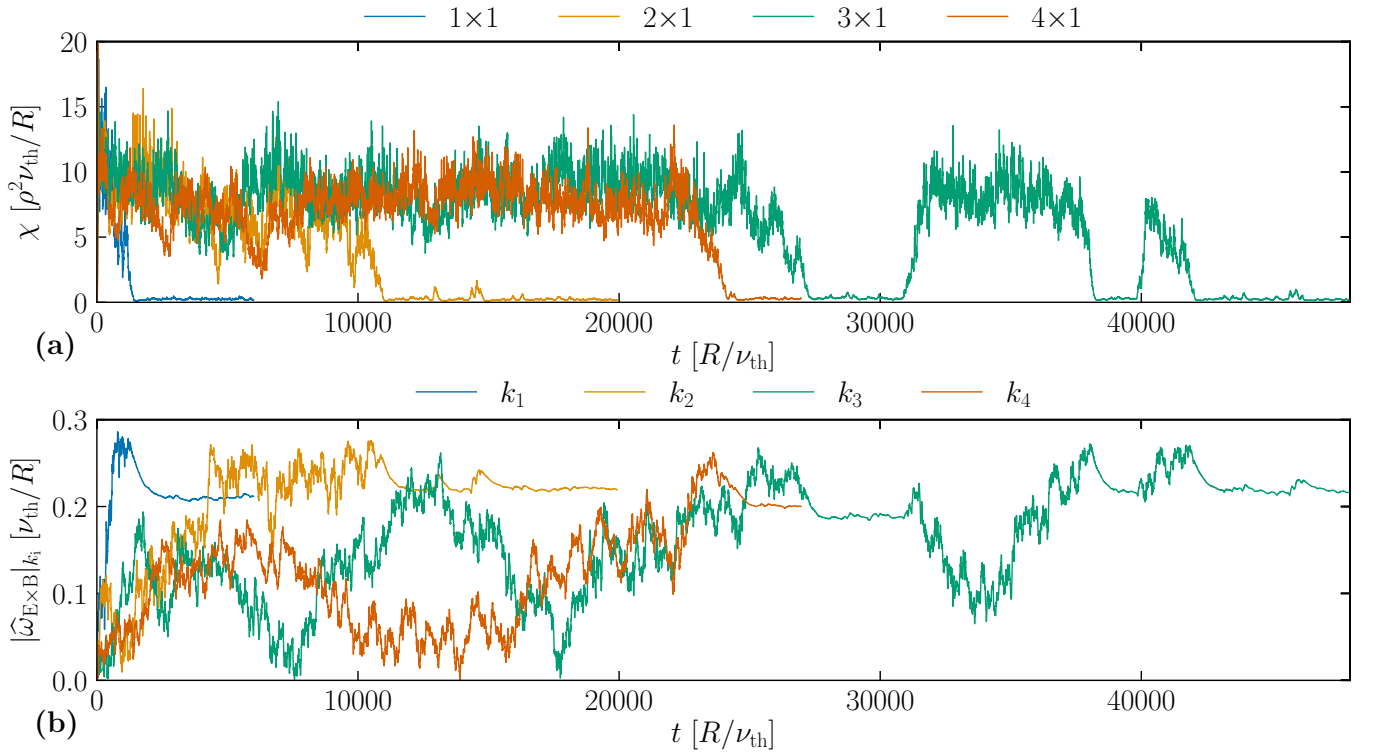


FIG. 2: (a) Time traces of the heat conduction coefficient  $\chi$  for  $R/L_T = 6.0$  for radial increased box sizes (b) Time traces of  $|\hat{\omega}_{E \times B}|_{k_i}$  for radial increased box sizes

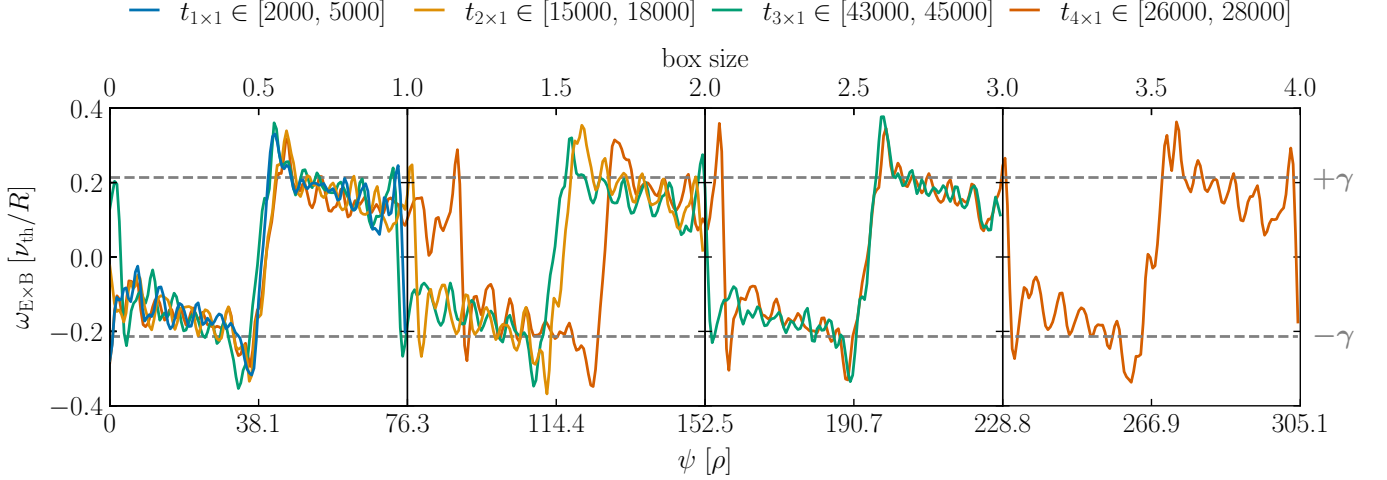


FIG. 3: Comparison of shearing rate  $\omega_{E \times B}$  for radial increased box sizes. The staircase structure got shifted for better visibility.

In the next step the box size was increased in radial and binormal direction at the same time. For this simulation the turbulence got stabilized and fully developed after 1500 normalized time unit seen in Fig. 4. This leads to a much faster computation of zonal flow structures if the box size had to be increased. In comparison, the box size  $3 \times 1$  gets stabilized and fully developed after 42000 normalized time units.

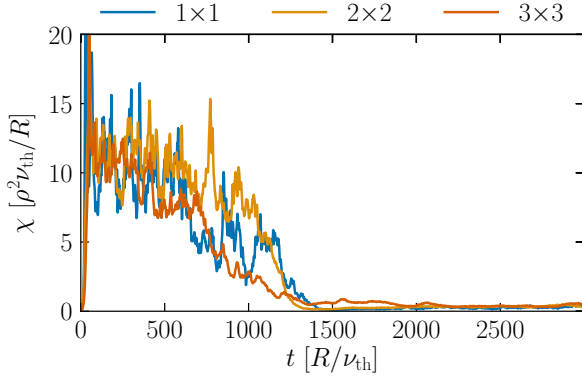


FIG. 4: Time traces of the heat conduction coefficient  $\chi$  for  $R/L_T = 6.0$  for radial and binormal increased box sizes

Even for this type of box sizes the wavelength converges with the box size and the Waltz rule is still satisfied. For the  $3 \times 3$  box size the  $E \times B$  staircase structure repeats itself four times which can be seen in Fig. 5. This stands in contradiction to the repetition of the radial increased box size. One could argue that the repetition of the staircase structure of a radial and binormal increased box size is greater equal  $N_R$ . This poses the question whether  $E \times B$  staircase structure has a different repetition for different box sizes, for different box sizes, but this will need further research to be conducted.

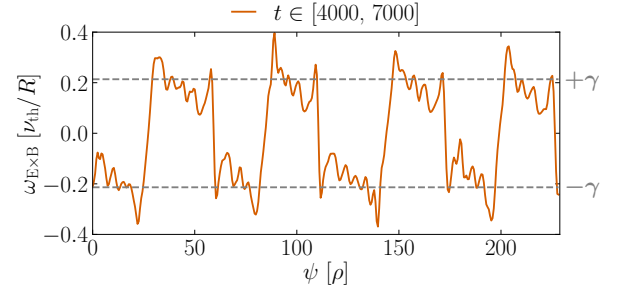


FIG. 5: Stabilized shearing rate  $\omega_{E \times B}$  for boxsize  $3 \times 3$

To conclude, the wavelength does converge with the chosen box size and the Waltz rule holds in every simulation. Long runs can produce stabilized turbulence. Further investigation of the long wavelength zonal mode has to be made to determine if and under what conditions the turbulence has been stabilized. Therefore, it is important that only one long wavelength zonal mode has a maximal amplitude for given wave vector  $k_i$  which is also the longest wavelength zonal mode. The  $E \times B$  staircase structure repeats itself multiple times in increased box sizes whereas radial increased box size shows a link between repetition and the times of radial box size increase, although this does not hold for radial and binormal increased box sizes.

#### DATA AVAILABILITY

The data that support the findings of this study are available from the corresponding author upon reasonable request.

- <sup>1</sup>A. G. Peeters, F. Rath, R. Buchholz, Y. Camenen, J. Candy, F. J. Casson, S. R. Grosshauser, W. A. Hornsby, D. Strintzi, and A. Weigl, “Gradient-driven flux-tube simulations of ion temperature gradient turbulence close to the non-linear threshold,” *Phys. Plasmas* **23**, 082517 (2016).
- <sup>2</sup>W. A. Cooper, *Plasma Physics and Controlled Fusion* **30**, 1805 (1988).
- <sup>3</sup>H. Biglari, P. H. Diamond, and P. W. Terry, *Phys. Fluids B: Plasma Physics* **2**, 1–4 (1990).
- <sup>4</sup>A. M. Dimits, G. Bateman, M. A. Beer, B. I. Cohen, W. Dorland, G. W. Hammett, C. Kim, J. E. Kinsey, M. Kotschenreuther, A. H. Kritz, L. L. Lao, J. Mandrekas, W. M. Nevins, S. E. Parker, A. J. Redd, D. E. Shumaker, R. Sydora, and J. Weiland, “Comparisons and physics basis of tokamak transport models and turbulence simulations,” *Phys. of Plasmas* **7**, 969–983 (2000).
- <sup>5</sup>T. S. Hahm and K. H. Burrell, “Flow shear induced fluctuation suppression in finite aspect ratio shaped tokamak plasma,” *Phys. Plasmas* **2**, 1648–1651 (1995).
- <sup>6</sup>K. H. Burrell, *Phys. Plasmas* **4**, 1499–1518 (1997).
- <sup>7</sup>R. E. Waltz, R. L. Dewar, and X. Garbet, *Phys. Plasmas* **5**, 1784–1792 (1998).
- <sup>8</sup>F. Rath, A. G. Peeters, R. Buchholz, S. R. Grosshauser, P. Migliano, A. Weigl, and D. Strintzi, “Comparison of gradient and flux driven gyrokinetic turbulent transport,” *Phys. Plasmas* **23**, 052309 (2016).
- <sup>9</sup>M. J. Pueschel, M. Kammerer, and F. Jenko, *Physics of Plasmas* **15**, 102310 (2008).
- <sup>10</sup>R. E. Waltz, G. D. Kerbel, and J. Milovich, *Phys. Plasmas* **1**, 2229 (1994).
- <sup>11</sup>G. Dif-Pradalier, P. H. Diamond, V. Grandgirard, Y. Sarazin, J. Abiteboul, X. Garbet, P. Ghendrih, A. Strugarek, S. Ku, and C. S. Chang, *Phys. Rev. E* **82**, 025401 (2010).
- <sup>12</sup>A. G. Peeters, Y. Camenen, F. J. Casson, W. A. Hornsby, A. P. Snodin, D. Strintzi, and G. Szepesi, *Comput. Phys. Commun.* **180**, 2650 (2009).